A NOVEL 1ST GENERATION COMPUTED TOMOGRAPHY SCANNER

By

Nicholas L. Kingsley

A thesis submitted in partial fulfillment of the
requirements for the degree of

Bachelor of Science

Houghton College

December 2003

Signature of Author……..……..
Department of Physics
May 19, 2003

……..
Dr. Ronald Rohe
Associate Professor of Physics

……..
Dr. Mark Yuly
Professor of Physics

A REDUCED EXPOSURE TRANSMISSION COMPUTED TOMOGRAPHY

By

Nicholas L. Kingsley

Submitted to the Department of Physics
on December 19, 2003 in partial fulfillment of the
requirement for the degree of
Bachelor of Science

Abstract

A preliminary design for a first generation tomography scanner is being designed and constructed. The scanner uses Na-22 as the radiation source, with annihilation photons being counted by shielded NaI detectors. The novel design of the scanner allows a very weak radiation source to be used by taking advantage of the back-to-back 511 keV annihilation photons emitted after Na-22 B^+ decay to improve the signal to noise ratio. The object being scanned will be translated and rotated systematically by computerized motor control using two motors attached to a standard rotary table.

Thesis Supervisor: Dr. Ronald Rohe
Title: Associate Professor of Physics

TABLE OF CONTENTS

Chapter 1 ..... **1**
- **1.1 Description of the Computed Tomography Scanner** **1**
- **1.2 History and Motivation** **2**
- **1.3 The Theory of Computed Tomography** **7**

Chapter 2 ..... **24**
- **2.1 The Differences** **24**
- **2.2 Apparatus** **26**

Chapter 3 ..... **31**
- **3.1 Detector Energy Resolution** **31**
- **3.2 Background Reduction** **33**
- **3.3 Collimator Efficiency** **42**
- **3.4 Data Collection Time** **44**

Chapter 4 ..... **50**
- **4.1 Summary and Observations** **50**

TABLE OF FIGURES

Figure 1. Compton Scattering……..7
Figure 2. Photoelectric effect……..9
Figure 3. Beam Attenuation……..10
Figure 4. Beam through two different materials……..12
Figure 5. Interaction Comparison……..13
Figure 6. First Generation Motion……..16
Figure 7. Coordinate Systems..……..19
Figure 8. Integral path selection……..20
Figure 9. Mechanical Schematic……..26
Figure 10. Collimator Mounting……..27
Figure 11. Electronic Schematic……..29
Figure 12. Detector #1 Energy Resolution……..32
Figure 13. Detector #2 Energy Resolution……..32
Figure 14. Na-22 Spectrum Requiring Coincidence……..32
Figure 15. Na-22 Spectrum Requiring No Coincidence……..34
Figure 16. Co-60 Spectrum Requiring No Coincidence..……..34
Figure 17. Co-60 Spectrum Requiring Coincidence……..35
Figure 18. Na-22 Spectrum Coincidence 0cm Water.……..36
Figure 19. Na-22 Spectrum No Coincidence 0cm Water……..37
Figure 20. Na-22 Spectrum Coincidence 5cm Water……..37
Figure 21. Na-22 Spectrum No Coincidence 5cm Water……..38
Figure 22. Na-22 Spectrum Coincidence 10cm Water……..38
Figure 23. Na-22 Spectrum No Coincidence 10cm Water……..39
Figure 24. Na-22 Spectrum Coincidence 13cm Water……..39
Figure 25. Na-22 Spectrum No Coincidence 13cm Water……..40
Figure 26. Graph With Slope Being Attenuation of Water……..41
Figure 27. Collimator Allignment……..43
Figure 28. Geometric Collimation……..44
Figure 29. Beam Overlap……..48

Chapter 1

INTRODUCTION

1.1 Description of the Computed Tomography Scanner

Computed Tomography is a method of constructing a three dimensional image of the internal structure of a solid body. This method uses computers to construct an image using information obtained from x-rays that have passed through the body from multiple angles. Although there are other methods of imaging internal structure that pre-date Computed Tomography, these methods have various disadvantages. Before Computed Tomography it was possible to image the tissue using only traditional radiographic imaging. Radiographic imaging is the type of 2-dimensional projection x-ray that would be used to diagnose a broken bone. This method is very much like taking a photograph. The attenuation of x-rays passing through the body is projected onto film and a two dimensional image is produced. As a result of the transfer from 3-D to 2-D the overlapping tissue can cause some critical details to be obscured.

Computed Tomography, on the other hand, allows a 3-D image to be constructed which reveals a much more detailed view without obstruction. This 3-D image begins with the construction of multiple 2-D images. Each of these 2-D images can then be stacked on top of one another in order to construct the full 3-D image. In order to

construct each of these 2-D images a beam of x-rays is transmitted through the body in an organized overlapping pattern of beam angles and translations. As the beam passes through the body x-rays are removed. The amount by which the x-rays are removed is determined by the attenuation coefficient of the material. The information obtained can then be evaluated and the attenuation coefficient calculated at each point on the object. The attenuation coefficient at each point is then assigned a value in order to represent its ability to remove x-rays from the beam. This value will correspond to a shade that will represent that value on the computer screen. For example darker gray might correspond to a high attenuation coefficient, which would correlate to a large removal of x-rays from the beam. The points would then be assigned a pixel on the computer screen where the assigned shade for each point is displayed. This spread of darker and lighter pixels on the screen reveals an image that can be used to distinguish between the different materials with different attenuation coefficients in the body. Our design differs from the standard Computed Tomography scanner in its ability to reduce the intensity of the radiation source needed to form the transmission beam.

1.2 History and Motivation

The first practical technique for imaging a solid body began at the discovery of the x-ray. The x-ray was discovered in the laboratory of Wilhelm Conrad Roentgen on

November 8, 1895. While testing the characteristics of high-energy cathode rays he stumbled upon an important discovery. At the time, he was hoping to isolate the rest of the room from any radiation that might be escaping from the cathode tube. This was done in order to isolate his experiments from outside influences. In doing so the tube was surrounded by dark cardboard in order to prevent any visible light from escaping. While testing the cardboard he noted a light glowing in the room. This glowing was coming from the fluorescence of a piece of paper that was coated with barium platinocyanide. He knew that the glowing could not be caused by electrons, which would be blocked by the glass tube surrounding the cathode, or by light which had been totally blocked by the cardboard. He realized at this point that it must be some unknown ray that was producing the fluorescence. While studying this new ray he found that by placing different objects in between the tube and the paper he could cause the brightness to be reduced by different amounts. This indicated that some objects would allow this new ray to pass through more easily than others. When he held his hand in between the tube and the paper he discovered the image of his skeleton was projected onto the paper.[1]

The discovery was of such importance and interest that it was shortly made public with its publishing on January 6, 1896. Very soon after the discovery of the x-ray it was possible to purchase x-ray emitting devices. Also around this time the discovery of gamma rays, beta particles and alpha particles were made. All of these discoveries were made in a short period of time after the discovery of the x-ray. Due to Roentgens interest in allowing others to access his discovery, these devices were available for extremely low cost. This low cost and availability allowed the development of x-ray use in diagnostics to appear very quickly. Incomplete understanding of the x-ray, however, caused some misuse and overexposure of operators to the radiation. Still, the use of x-rays quickly developed the methods of x-radiography and a new diagnostic tool was available.

Although x-radiography was used for many years to diagnose many different ailments the method left much information unattainable. One disadvantage was that the representation of a three dimensional body by a two dimensional image meant certain information could not be observed due to intrinsic obstructions. Also, subtle differences in contrast were not visible in the image due to the inability to resolve these small differences in attenuation and x-ray scatter resulting from the large-area x-ray beams used in conventional radiography.

The disadvantages of radiography left much room for a new imaging technique to be developed. The ideas surrounding a new development in medical imaging began to arise fairly soon after the discovery of the x-ray. New techniques would include Magnetic Resonance Imaging (MRI), which involves relaxation properties and resonant frequencies of a nucleus, properties that depend on the nucleus' environment. Since the magnetic resonance depends on what type of environment the nucleus is in, a magnetic resonance signal will vary according to its specific biological surroundings.. These signals can be measured in order to create an image of the different materials in the body. Another imaging technique is ultrasound, which uses high frequency sound waves to construct an image.

One of the new developments would one day be called computed tomography, however, long before the name was coined, certain contributing ideas began to lay the foundation. One such idea was related to the image reconstruction mathematics that would be needed in order to make computed tomography possible. A mathematician named J. Radon, while working with gravitational theory, proved that any three-dimensional object could be reconstructed from an infinite set of all its projections.2 Radon is also credited with using a turntable and x-ray projections to make predictions about the internal structures of a phantom head that was constructed of a bed of nails.3

After the development of such mathematics many different scientists working toward totally different goals began to develop its practical use and as a result, contributed to the pool of ideas used to develop computed tomography. Bracewell, in 1956 used ray projections to construct a solar map in his field of radio astronomy. Many scientists throughout the 1960's realized the practical implications that computed tomography might have on medicine and as a result began work on reconstruction tomography theory as well as plausibility experimentation. Cormack for instance has written of his own work with an experimentally operating computed tomography scanner in 1963. Other Russian scientists are noted to have had even earlier experimental computed tomography scanners using analogue reconstruction methods and x-ray fan beams as the source of radiation. These experiments were performed by Korenblyum (1958) and Tetel'Baum (1957). 4Although the development of computed tomography is very much spread out among a diverse group of scientists two in particular, Hounsfield and Cormack, shared the Nobel Prize of Physiology and Medicine for their contributions to the particular development of a commercially practical scanning device.

The computed tomography scanning device that is being constructed in this project differs in the amount of radiation required. The hope is that by reducing the required amount of radiation we could reduce the dosage and also reduce the amount of precaution necessary to run the computed tomography scanner, such as lead shielding. This might allow computed tomography to become a diagnostic tool for medical doctors working in underdeveloped environments since the design will cause a reduction in the price of the scanner. This scanner might also be better for research questions concerning image reconstruction.

This computed tomography device is being designed as a first generation scanner with modifications in the type of radiation being used, electronics setup and the rotation and translation technique. The first generation computed tomography scanner has an inline x-ray tube and detector setup that rotates around the object being scanned. In

this project, however, the object is rotated instead of the entire detector-radiator system. The type of radiation being used will not be an x-ray tube but will be an indirect byproduct of Na-22 B^+ decay. This source emits positrons which rapidly annihilate with atomic electrons that result in the emission of 2 back-to back 511 keV annihilation photons that can be used to electronically require coincidence between gamma detections and therefore reduce background radiation being detected. The reduction of background radiation allows the radiation source to be less active since the signal does not need to compete with background noise.

The advantages of the scanner include lower cost and that it would be more portable. The low cost of the scanner would allow field doctors in remote areas or third world hospitals to purchase the scanner when conventional scanners would be far too expensive. Also, the relatively small size and lack of lead shielding required by the scanner would allow it to be transported by field doctors to remote areas. Another advantage of this design might be the source of radiation that is being used. This design will implement annihilation photons instead of x-rays. The source of the annihilation photons that are used in this design is a small radioactive Na-22 source that could be easily transported to the field.

The disadvantages might include the higher energy annihilation photons involved and the more complicated electronics for each in-line detector channel. The more complicated electronics would make repair more difficult for field doctors to perform. The imaging time would also be very slow compared to modern-day scanners.

1.3 The Theory of Computed Tomography

Computed tomography is a method that evaluates the information obtained from multiple x-ray transmission beams that have passed through the body being scanned in order to compute an image. The information obtained from each transmission beam of x-rays is a measurement of the amount by which the beam intensity has decreased due to interaction with the different materials in the body. These interactions reduce the intensity of the beam by removing some of the x-rays from the beams' path. There are three interaction mechanisms that will remove x-rays from a beam that is traveling through a material, Compton scattering, the photoelectric effect and pair production. The x-ray is a particular form of electro-magnetic radiation and therefore can be treated as a wave or a particle called a photon. The photon, carries both energy and momentum. In the Compton effect, a photon (x-ray), of energy E, travels through the material until it strikes an atomic electron.

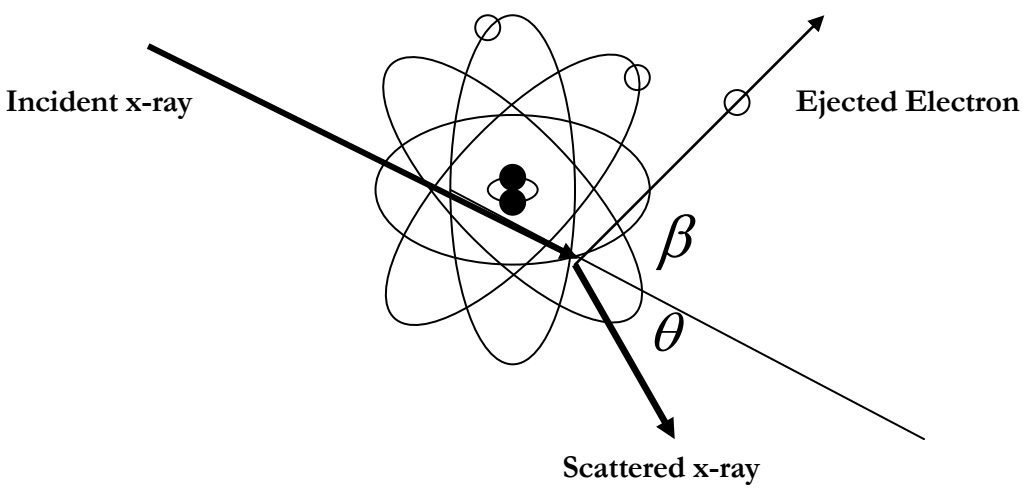

Figure 1.3.1 Figure demonstrating Compton scattering. Showing the incident x-ray interacting with an atomic electron and ejecting it at angle beta with an x-ray scattered at angle theta.

Some of the momentum of the photon is transferred to the electron, which is thrown from the atom at an angle β relative to the direction of the original photon. The photon, as a result of striking the electron, loses energy and changes direction. This change in direction has removed the photon from the x-ray beam and it will not be detected as part of the beam. The photon has a new energy, E and is deflected from its original direction by the angle θ. This x-ray may actually be detected by the detector but will not be considered part of the beam in data analysis since it no longer carries the same energy as the other photons in the beam. Using relativistic conservation of energy and momentum the energy of the deflected x-ray is $\frac{E_0}{1+\frac{E_0}{M_e c^2}\left(1-Cos(\theta)\right)}$,

where m_e is the mass of the electron and c is the speed of light. 5

The photoelectric effect occurs when the incident photon strikes an electron and transfers all of its energy and momentum to an electron. In doing so the x-ray is completely absorbed and therefore will not be detected. The electron will require a

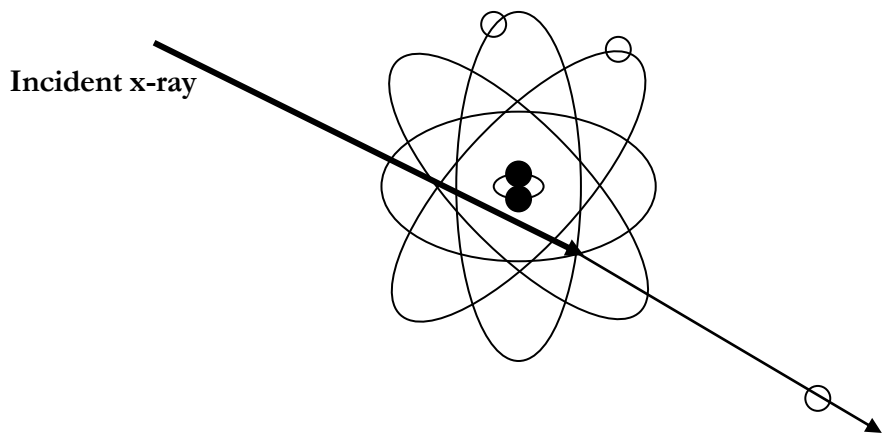

Figure 1.3.2 Figure demonstrating Photoelectric effect.
The incident x-ray collides with an atomic electron and
ejects the electron.

particular energy ϕ to be deposited in order to remove it from the atom that it is a part of. We know that the energy of the incident photon is equal to hf, where h is Planck's constant and f is the frequency of the incident x-ray. The kinetic energy of the ejected electron will be equal to the difference in incident photon energy and ϕ.6

Pair production occurs when the photon is changed into an electron and a positron. This phenomenon must occur very near a nucleus (or rarely atomic electron) in order to conserve momentum. Pair production requires photons with energies of at least 1.02 MeV. This particular interaction will not occur in our design since photon energy will not be high enough for pair production. [7,8]

The attenuation of a beam of x-rays through a material can be calculated. It can be assumed that a small thickness of material Δx, will reduce the intensity of the beam by an amount $I(x)-I(x+\Delta x)$. Where $I(x)$ is the beam intensity a distance x through the material and $I(x+\Delta x)$ is the beam intensity a distance $x+\Delta x$. $I(x)-I(x+\Delta x)$ is proportional to both the intensity of the beam as it reaches the material and the thickness of the material. So

$$I(x)-I(x+\Delta x) \propto \Delta x I(x) \quad (1.1)$$

$$I(x)-I(x+\Delta x) = \mu \, \Delta x I(x) \quad (1.2)$$

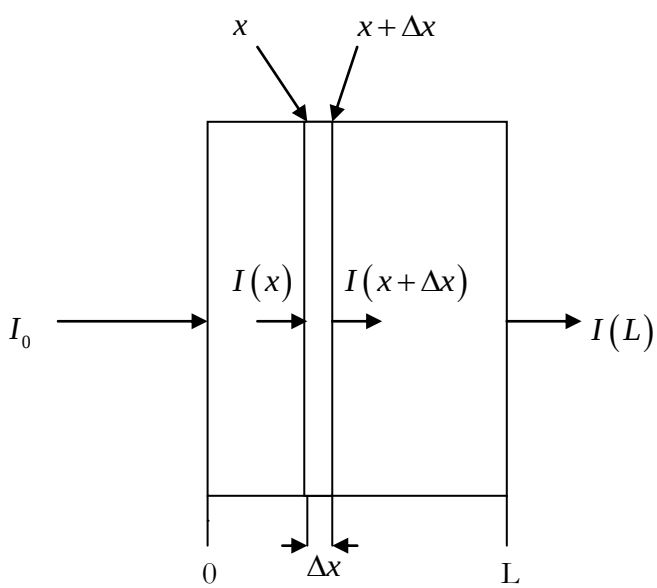

Figure 1.3.3 Figure demonstrating the attenuation of a beam through distance dx of a material.

From this the definition of a derivative can be used.

$$\frac{I(x)-I(x+\Delta x)}{\Delta x}=\frac{-dI}{dx} \quad (1.3)$$

$$\frac{-dI}{dx}=\mu I(x) \quad (1.4)$$

$$-dI=\mu I(x)dx \quad (1.5)$$

Where μ is a proportionality constant. Solving for I can be done by integrating this equation. The intensity will be integrated from its original intensity I_0 to the beam intensity after it has traveled through x distance of the material, I. The thickness will be integrated from 0 to a distance x into the material, the point at which we wish to know the beam intensity. This results in the integral

$$\int_{I_0}^{I}-\frac{dI}{I(x)}=\int_{0}^{x}\mu dx \quad (1.6)$$

Solving gives ln I – ln I_0 = - μ x, which when simplified is $I=I_0e^{-\mu x}$. This is called Beer's Law.

The constant μ is dependent on the nature of the beam and material. This constant is our linear attenuation coefficient, so we have the equation $I=I_0e^{-\mu x}$. This equation assumes a homogeneous medium. This is rarely the case and is especially not the case when working with computed tomography. However, if the x-ray is incident along a line through the body in which there are two different kinds of materials then the

beam intensity calculation is simply $I = I_0 e^{-(\mu_1 x_1 + \mu_2 x_2)}$ where x_1 and x_2 are the distances through which the beam travels through the material of attenuation coefficient μ_1 or μ_2.

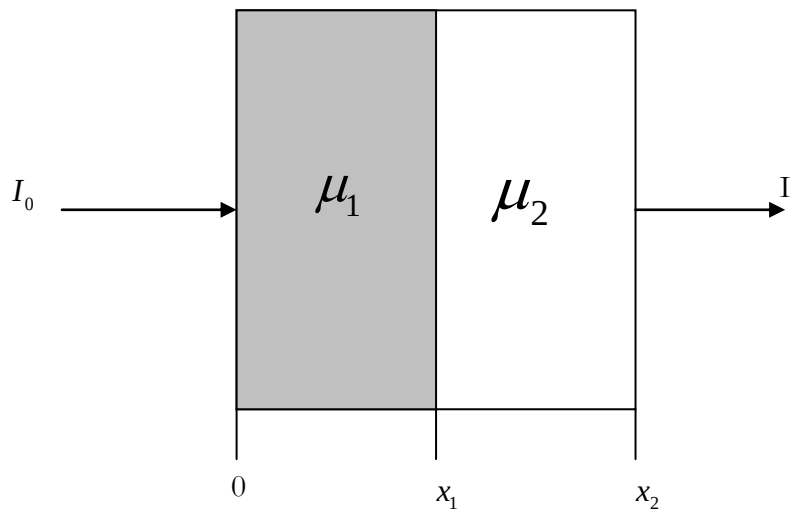

Figure 1.3.4 Figure demonstrating the attenuation of a beam traveling through two different materials with different attenuation coefficients.

In the case of n different materials in the line of transmission $I = I_0 e^{\sum_{i=1}^{n} \mu_i x_i}$,where x_i is the distance through which the beam passed through a material of linear attenuation coefficient μ_i.

Different materials exhibit different x-ray attenuation. Also the x-ray energy will affect the probability of interaction with any given material. Each of the interacting

mechanisms has incident beam energy ranges at which the net effect of the mechanism is most proficient.

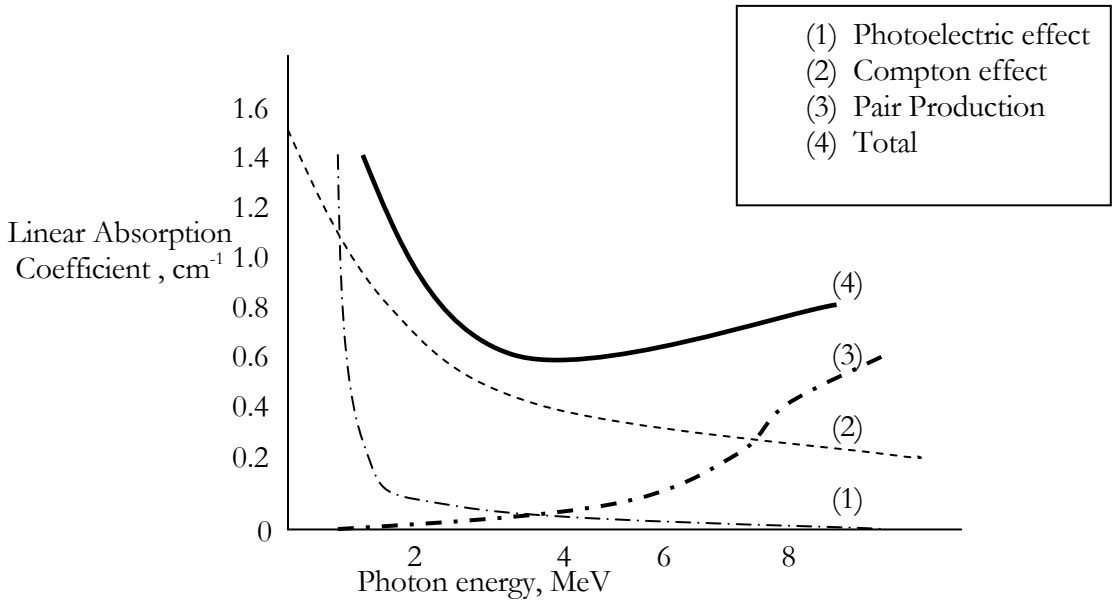

Figure 1.3.5 Figure demonstrating the attenuation of a beam due to the different interactions. This is the theoretical linear absorption coefficient of lead.

The photoelectric effect will remove more x-rays from an incident beam than the Compton effect for lower energy x-rays up to 0.1 MeV energy. At 0.1 MeV the Compton effect will become more proficient than the photoelectric effect at removing x-rays from an incident beam. Pair production takes on a minor roll in removing x-rays from a beam at lower to medium energies. Pair production will begin to remove x-rays from a beam with energy at about 1.02 MeV and at an incident beam energy of about 5

MeV will remove more x-rays then either the photoelectric effect or Compton scattering. The amount by which a material tends to remove x-rays from a beam that is traveling through it is called the linear absorption coefficient and is signified by μ. The numerical value that is assigned to μ will depend not only on the absorptive properties of the material but also on the energy or wavelength of the x-ray incident on the material. The relationship between the wavelength, λ of the incident x-ray and variation in μ is approximated to be proportional to λ^3.[9]

In computed tomography the interest is directed more toward the change in linear absorption coefficient as a result of the properties of the material. By using a mono-energetic x-ray beam, we can assume that changes in μ will be a result of the characteristics of the material that the beam is traveling through. The linear absorption coefficient greatly depends on the mass density ρ of the material that it is traveling through. The higher ρ is the more the beam will be attenuated through the material and the higher μ will be.

The quantity $\frac{\mu}{\rho}$ is known as the mass absorption coefficient. This mass absorption coefficient will vary little with the mass density of the material which will allow us to study different aspects of the material that will effect μ. The mass absorption coefficient will vary proportionally with x-ray wavelength cubed, as we have already discussed, and with the atomic number cubed of the material being traversed. This variance with atomic number is a result of the number of electrons that are available in the material to interact via the photoelectric effect, the Compton effect or elastically. Materials with a high atomic number (Z) will have a very positively charged nucleus and will therefore have many orbiting electrons in order to render the atom electrically neutral.[10]

Using the fact that the x-ray beam will be attenuated more readily by materials with high Z and high ρ, we can see that the linear coefficient of attenuation, μ would be useful in determining what types of materials are being traversed by the x-ray beam. The mass absorption coefficient varies proportionally with the materials Z and with the incident x-rays λ by the equation $\frac{\mu}{\rho} = k\lambda^3 Z^3$ where k is a constant of proportionality. Holding the wavelength of the x-ray constant and allowing the product $k\lambda^3$ to become the constant l, the linear absorption coefficient can be expressed by the equation $\mu = lZ^3\rho$. It should be noted that the constant k is not held precisely constant given multiple variations in x-ray energy and material composition but changes only slightly in comparison to the other components that cause change in μ and can therefore be held as a constant for most applications.[11]

The dependence of μ on both the atomic number of the material and the mass density allows an x-ray transmission through an object to distinguish both a difference in atomic structure of a material and the density of the material. For example an x-ray transmission through water would reveal a difference in μ from an x-ray transmission through steam even though the atomic number of the material remained constant through each of the x-ray transmissions. Also if two materials with similar mass densities but different Z numbers are examined by an incident x-ray transmission the μ will be affected by the difference in Z number.

With a single transmission beam the different linear attenuation coefficients along the transmission line through the object cannot be determined, however with multiple transmission lines through the same plane but at different angles and positions calculations can be made that will allow the linear attenuation coefficients to be determined. A computed tomography scanner uses a systematic approach to obtain multiple perspectives of each point on a plane of the object. The data from each

perspective can be collected and calculations made using the data that will allow the linear attenuation coefficient at each point to be found. A first generation computed tomography scanner rotates and translates an in-line detector and x-ray source around the object being scanned while making multiple transmission measurements for every angle that is turned by the system.

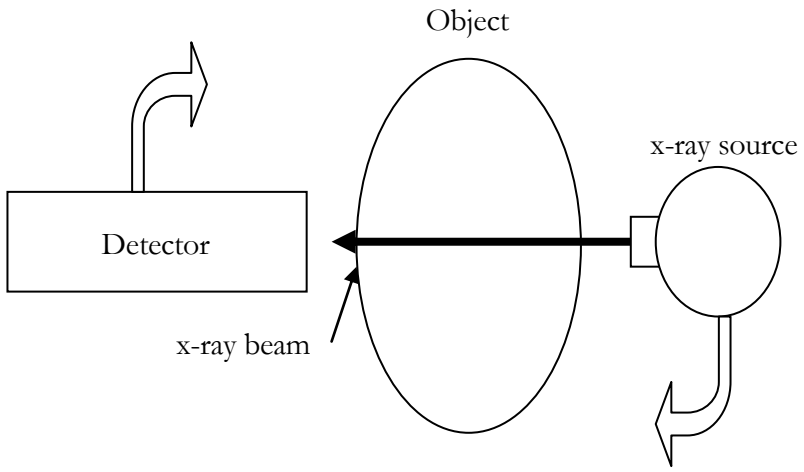

Fig 1.3.6 Figure representing the motion of a First Generation Computed Tomography Scanner. The object remains fixed while the x-ray source and detector rotates and translates around it.

This method systematically collects the data needed to calculate the linear attenuation coefficient for every point on the object. Typically 180 angle settings and 160 translational settings for each angle are used. This results in $180 \cdot 160 = 28{,}800$ measurements.

These data are then used to make calculations that will assign each pixel on a computer screen with a particular shade of gray that corresponds to the value of the linear attenuation coefficient at the point in the object that the pixel is representing. This point on the object is called a voxel and actually represents the average value of μ in a particular volume element of typical dimensions $3\text{mm} \times 3\text{mm} \times 10\text{mm}$. For the planar scan where a plane through the object is being viewed, the $3\text{mm} \times 3\text{mm}$ face is what is imaged and represented as a pixel on the computer screen. This distribution of shaded pixels will then appear as an image that will accurately represent the shapes and positions of different components contained in the object being scanned. The algorithms used to calculate the shades that should be assigned to each pixel on the computer screen are called reconstruction algorithms. There are four basic types of reconstruction algorithms.

The first is Simple backprojection. In this method the body being scanned is divided into volume elements each of which is assumed to contribute to the total attenuation of the beam equally. By summing all of the attenuations that intersect at one particular element the attenuation coefficient can be determined for that element. When this is done for all of the elements in the object a composite image of attenuation coefficients is constructed. This method is very straightforward but is also rarely used since the image produced is blurred.

The second and most frequently used reconstruction method is the filtered backprojection method. This method is also called the convolution method. This method uses a one-dimensional integral to reconstruct the image. In this method a deblurring function is combined with the x-ray transmission data in order to remove the blurring before the data are backprojected.

The third method is the Fourier Transform convolution method. In this method the x-ray transmissions for each angle are separated into frequency components of different amplitudes. From these components the image is constructed in "frequency space" and then transformed to a "position space" image on the computer screen by an inverse Fourier transform.

The fourth reconstruction algorithm is the series expansion. In this method the x-ray attenuation data for a particular angular orientation are divided into equally spaced elements along each of several rays. These data are then compared to the data of the same element but at different angular orientation. The difference in attenuation then allows the element to be assigned a different value. [12]

What follows is a derivation from reference [13]. The convolution method is an extension of the calculation used to find the intensity of the beam (Beer's Law) after it has been transmitted through an object, which takes into account the spatial distribution of μ. This equation is

$$I_{\phi}(x') = I_{\phi}^{0}\exp\left(-\int_{AB}\mu\left[x,y\right]dy'\right) \quad (1.7)$$

The x, y coordinate system remains constant with the object and the x', y' coordinate system rotates around the object according to ϕ. $\mu[x,y]$ is the two-dimensional distribution of the linear attenuation coefficient, ϕ and x' define the position of the measurement and $I_{\phi}^{0}(x')$ is the unattenuated intensity. The square brackets of $\mu[x,y]$ indicate a rectangular coordinate system. The detector will translate along x' and rotate according to ϕ. Also the bounds on the integral A and B are the entry and exit points respectively of the x-ray beam.

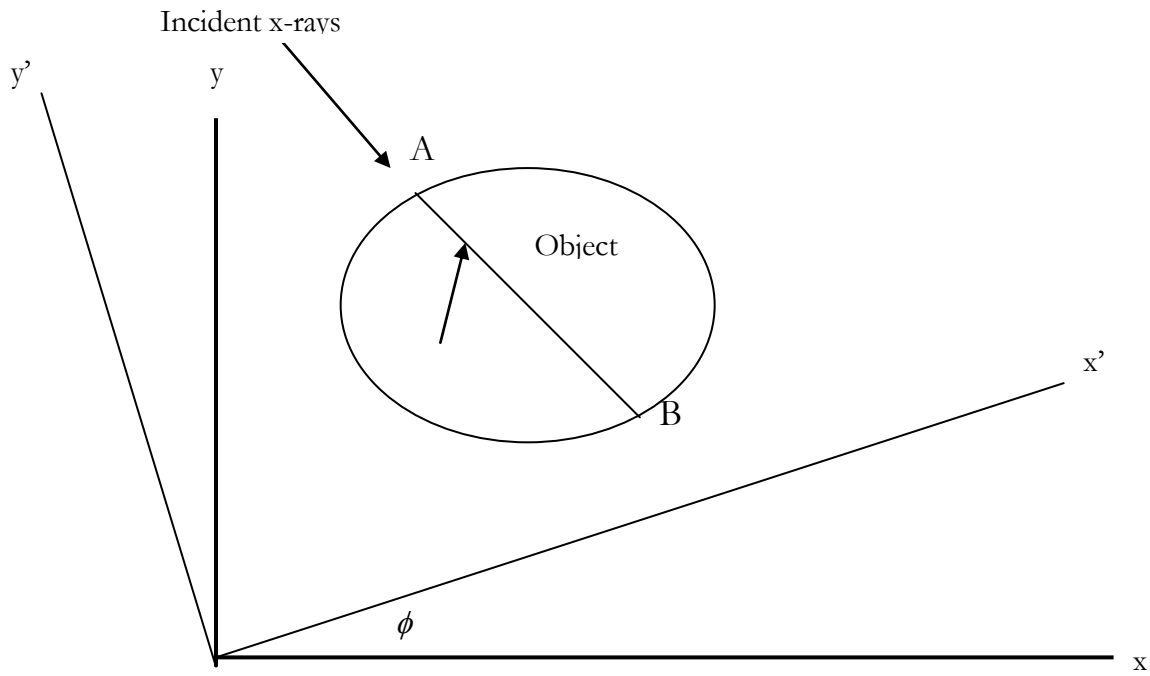

Fig 1.3.7 Figure showing the rotating and stationary coordinate systems used to describe the detector, projection ($\lambda_\phi(x')$) and voxel ($\mu[x,y]$) positions with respect to one another.

Next there must be an equation that relates the object function $\mu[x,y]$ and the measured projection data. The object function $\mu[x,y]$ is the variable that must be found. It is the attenuation coefficient at point x,y in the objects coordinate system. A single projection of the object is known as $\lambda_\phi(x')$, where the subscript ϕ defines the angle of the x-ray transmission and x' defines the translational position along the angle.

$\lambda_\phi(x')$ is defined to be equal to $-\ln\left(\frac{I_\phi(x')}{I_\phi^0(x')}\right)$, which by arrangement of our extension of Beers law is equal to

$$\lambda_\phi(x') = -\ln\left(\frac{I_\phi(x')}{I_\phi^0(x')}\right) = \int_{-\infty}^{\infty}\int_{-\infty}^{\infty} \mu[x,y]\delta\left(x\cos\phi + y\sin\phi - x'\right)dxdy \quad (1.8)$$

The Dirac delta function selects the path of the line integral to be the line along which the x-ray is transmitted since the equation of the line AB through the object is x'=xcosϕ +ysinϕ. When the contents of the Dirac delta function are equal to zero the integral of the function is equal to 1, however when the contents of the Dirac delta function is anything but zero the integral is equal to zero.

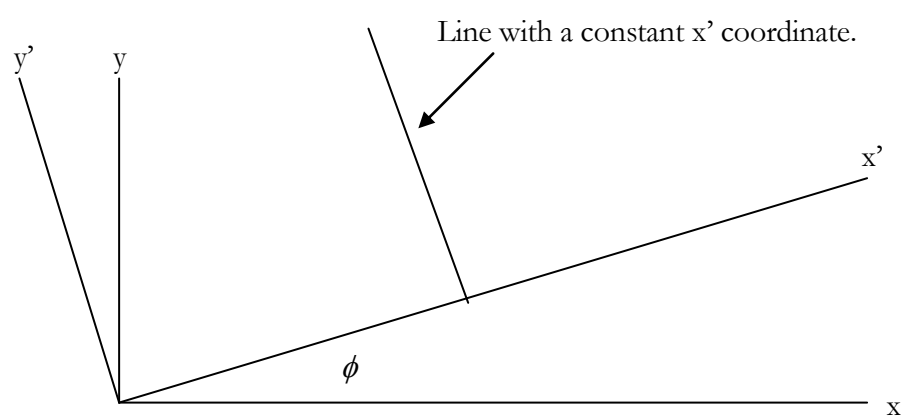

Fig 1.3.8 Figure showing the integral path selection. Along the x' line $x\cos\phi + y\cos\phi$ will be equal to x'. The Dirac delta function can then be used to only consider the line with a constant x' in the equation thereby selecting a projection line.

In order to obtain $\mu[x,y]$ from a set of projections this equation is inverted. The two-dimensional inverse polar Fourier transform that gives $\mu[x,y]$ is…

$$\mu^p(r,\theta)=\int_0^{\pi}\int_{-\infty}^{\infty}M^p(\rho,\phi)\exp\left[2\pi i\rho\left(x\cos\phi+y\sin\phi\right)\right]|\rho|\,d\rho d\phi \quad (1.9)$$

Where $\mu^p(r,\theta)$ is the polar coordinate representation of the two dimensional linear attenuation coefficient, $M^p(\rho,\phi)$ is the Fourier transform of $\mu^p(r,\theta)$. When this equation is broken into two parts

$$\mu[x,y]=\int_0^{\pi}\lambda_\phi^\dagger(x')\,d\phi\,|_{x'=x\cos\phi+x\sin\phi} \quad (1.10)$$

Where…

$$\lambda_\phi^\dagger(x')=\int_{-\infty}^{\infty}M^p(\rho,\phi)|\rho|\exp\left[2\pi i\rho x'\right]d\rho \quad (1.11)$$

This equation is the one dimensional Fourier transform of the product of $M^p(\rho,\phi)$ and $|\rho|$, so it is also possible to write it as the convolution of the Fourier transforms of both $M^p(\rho,\phi)$ and $|\rho|$. The Fourier transform of $M^p(\rho,\phi)$ is known to be the projection data $\lambda_\phi(x')$.

Next consider the Fourier transform of $|\rho|$. This function does not behave in such a way that its Fourier transform can exist, however due to limits imposed by the measurement system it is known that $M(\rho,\phi)$ has a maximum frequency component $\rho_{\max}$, therefore $|\rho|$ can be similarly truncated. So there is the transform p(x') of $P(\rho)$, where

$$P(\rho) = 0 \qquad |\rho| \geq \rho_{\max} \quad (1.12)$$

$$P(\rho) = |\rho| \qquad |\rho| \leq \rho_{\max} \quad (1.13)$$

Taking the Fourier transform.

$$p(x') = \int_0^{\rho\max} \rho \exp(2\pi i \rho x') d\rho - \int_{-\rho\max}^{0} \rho \exp(2\pi i \rho x') d\rho \quad (1.14)$$

Evaluating gives the result.

$$p(x') = \rho_{\max}{}^2 \left[2\mathrm{sinc}(2\rho_{\max} x') - \mathrm{sinc}^2(\rho_{\max} x') \right] \quad (1.15)$$

Using the convolution theorem $\lambda_\phi{}^\dagger(x')$ can be written as…

$$\lambda_\phi^\dagger(x') = \int_{-\infty}^{\infty} \lambda_\phi(x) p(x' - x) dx \quad (1.16)$$

Where $p(x' - x)$ is a filtering operation that corrects the blurring problem of the simple backprojection method. The dagger (†) indicates that the function is a filtered backprojection because the original projection is convolved with the $p(x' - x)$ filtering function. So the total solution is…

$$\mu[x, y] = \int_0^{\pi} \int_{-\infty}^{\infty} \lambda_\phi(x) p(x' - x) dx \quad [14] \quad (1.17)$$

With multiple x-ray transmission beams this equation can be used to determine the assigned linear attenuation coefficient for each pixel on a rectangular coordinate screen. When this is done the pixels are assigned shades of gray that correspond to the linear attenuation coefficient that they have been assigned. This produces an image.

Chapter 2

OUR DESIGN

2.1 The Differences

The new design that is being built differs from most other 1st generation computed tomography scanners in both the radiation source and the translation and rotation method. First, most computed tomography scanners use x-rays generated by use of a hot cathode x-ray tube. These x-rays are collimated to produce a beam. The new design however will not use x-rays but annihilation photons produced by a Na-22 source. Na-22 nuclei change into Ne-22. The energy transition that is being made is a 1.274 MeV gap that must be jumped by emitting a 1.274 MeV particle. 90.05% of the time the Na-22 nucleus emits a 1.274 MeV positron. The Na-22 will also emit a 1.274 MeV gamma ray in order to make the transition. The positron is the antiparticle of the electron. Since the environment around the decaying Na-22 contains atomic electrons the positron will almost immediately come into contact with an electron, which will slow the positron down by ionizing. The positron will then be captured to form positronium. The life of positronium, however, is very short and the two decay when the positron and electron annihilate into two or three annihilation photons.15 In order to conserve momentum the two annihilation photons must travel in opposite directions and must carry the same amount of energy. This positron-electron annihilation results in the production of two back-to-back 511 keV annihilation photons. We can use this fact to our advantage when building a computed tomography scanner. The Na-22 radiation source will emit annihilation photons in all directions, but by placing a collimator in front of the detector a narrow beam is produced that will travel through the object. Each annihilation photon that reaches the detector through

the collimator has a annihilation photon traveling in the opposite direction. By placing another detector behind the Na-22 source and directly across from the data detector and electronic setup can be built that will require a coincidence between a transmitted annihilation photon and the corresponding annihilation photon traveling in the opposite direction. In requiring such a coincidence the majority of background events can be eliminated. Instead of requiring a very intense x-ray source to produce a useable signal to noise ratio by enhancing the signal, the signal-to-noise ratio is maintained by reducing the background noise. Therefore a weaker and safer source can be used.

Another difference in the new design is the way the transmission beam is being rotated and translated across the object. In most computed tomography scanners to allow the object being scanned must remain motionless. This is a requirement for example if the object is a human. However, since our preliminary design will not be used on humans the object itself will be rotated and translated. This change simplifies the mechanical apparatus since it requires only one object to move rather then rotating and translating both the detectors and the source.

2.2 Apparatus

The apparatus is made up of two primary components, the motion setup and the detector setup.

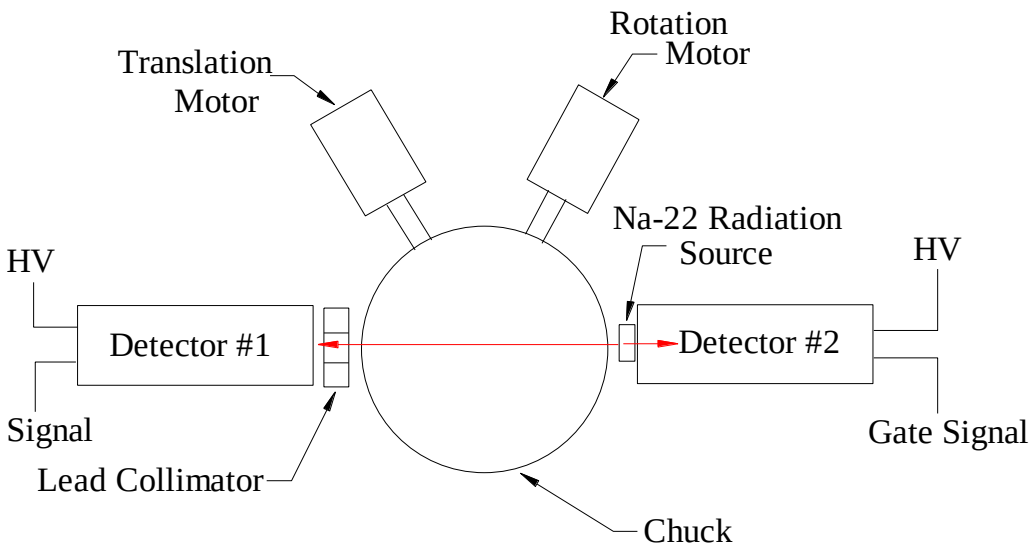

Fig 2.2.1 Mechanical schematic of the preliminary back-to-back annihilation photon computed tomography scanner. Shown are the motors used to move the chuck and therefore the object, as well as the detectors, collimator and Na-22 source.

For the motion setup there are two motors attached to a chuck. The object being scanned will be placed on the chuck and the motors will control its motion. One of the motors will control the rotation of the chuck and therefore the rotation of the object. The other motor that is attached to the chuck will control the objects translation. For every degree of rotation there will be a set of translations made. There is also a one micro-curie Na-22 source that will be used to emit the back-to-back 511 keV annihilation photons that make up the beam. This source is placed in front of detector

number two as shown in the figure. The annihilation photons collected by detector number two will allow the transmitted annihilation photons to be collected by detector number one. There are also two detectors. Detector number one is used to collect the radiation that has been transmitted through the object. The energy of the radiation is collected and stored as a spectrum in a multi-channel analyzer. Detector number two collects the corresponding radiation and causes a gate to allow the data being collected by detector number to be passed into the multi-channel analyzer. The collimator is used to narrow the number of annihilation photons being collected to those that are along a particular line through the object. The width of the collimator will determine the resolution of the image being produced. This setup has a collimator that is made up of 1 cm of lead through which there is a 1cm diameter collimation hole. This was made to fit onto the front of two lead bricks used for shielding detector number two from background radiation.

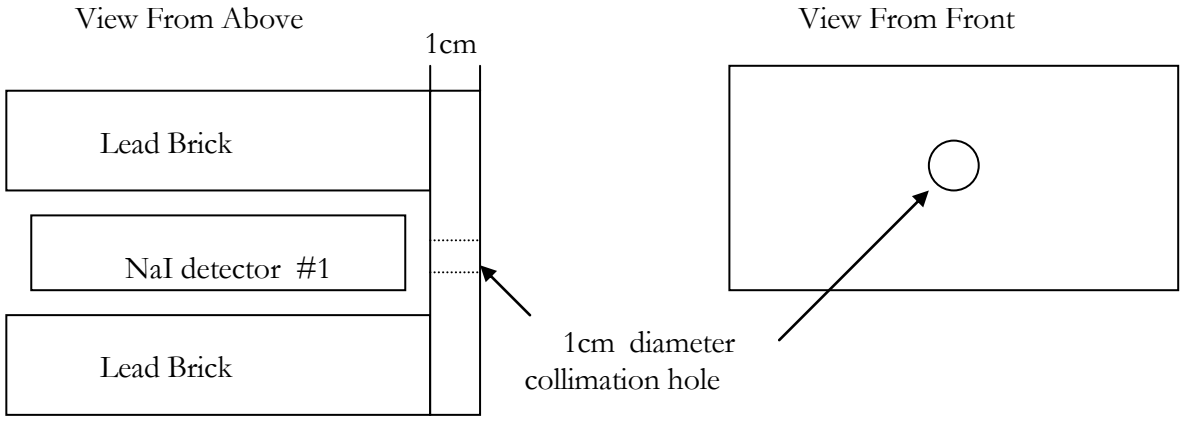

Fig 2.2.2 Figure demonstrating the mounting and dimensions of the lead collimator that forms the 1cm annihilation photon beam Also shown are the lead bricks used to eliminate some background radiation from detector number 2.

NIM electronics will be used to detect the coincidence between the 0.511 Mev annihilation photons. This circuit will allow only annihilation photons that are detected by detector number one in coincident timing with a 511 keV annihilation photon detection by detector number two to be collected and stored as a spectrum. The detectors are both NaI scintillating crystal detectors. These inorganic crystals are activated with an impurity of thallium, which provides luminescence centers in the band gap. Electrons raised from the valence band of the crystal, themselves excite an electron in a luminescence center. The excited luminescence center electron then falls back to its original non-excited state emitting radiation that is of a lower energy than the detected radiation. Since the wavelength of this radiation is longer than the original the scintillating crystal is usually transparent to it and the radiation is passed to the photomultiplier. The NaI detector is especially proficient at detecting gamma rays due to the crystals high-density structure.[16] The ratio of light emitted by the NaI crystal that has a thallium impurity is one photon per 50 eV of energy. So, the intensity of the light emitted to the photomultiplier is directly proportional to the energy lost by the incident radiation. The purpose of the thallium impurity in the NaI crystal is to make it more transparent to the emitted photon resulting from scintillation. A significant fraction of these photons reach the photomultiplier that focuses them to strike a photocathode. As the photons strike the photocathode they eject electrons that are collected and focused to multiple dynodes each with a higher potential that causes a multiplication of electrons to be emitted from each one. This results in a signal that is strong enough to be used but also is proportional to the energy of the incident radiation.17

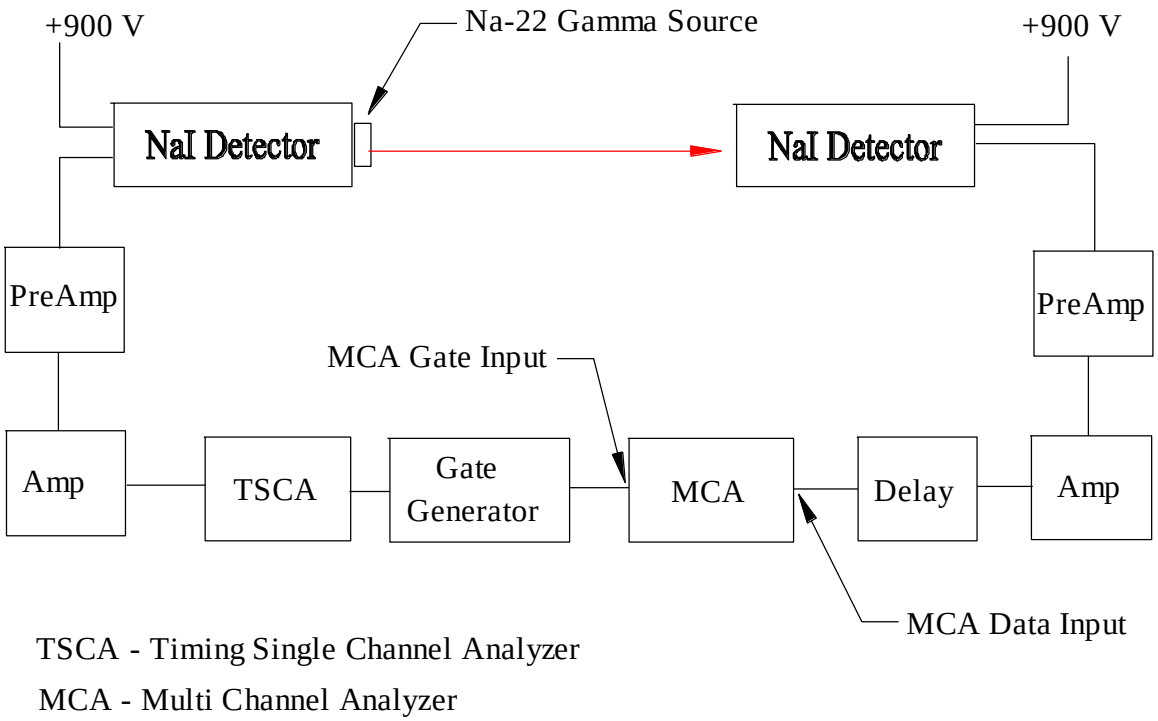

Figure 2.2.3 Schematic of the electronic circuit involved in data collection. These electronics allow the data collected by detector number two to be selected filtering out the detection of background events.

The detector number 2 collects the annihilation photons transmitted through the object and sends a current pulse to the preamplifier. This detector operates at 900 volts. The preamplifier, shapes and amplifies the signal for the spectroscopy amplifier. The spectroscopy amplifier amplifies and shapes the pulses, producing positive 0-10V pulses. The delay amplifier delays the signal in time so that it will reach the multi-channel analyzer at the same time as the gating signal sent by detector number 2. If the signals were sent directly from both detectors to the multichannel analyzer they would reach it at about the same time however the electronics involved in processing the

signal from detector number one will cause a significant time delay. The signal from the delay amplifier is input to the multichannel analyzer, which digitizes the pulse height and records the energy spectrum.

Detector number one collects 0.511 Mev annihilation photons in coincidence with the transmitted radiation. This detector also operates at 900 volts. The preamplifier, shapes and amplifies the signal for the spectroscopy amplifier. The spectroscopy amplifier amplifies and shapes the pulses, producing positive 0-10V pulses. The signal then reaches the Timing Single Channel Analyzer which produces a logic pulse for incident 0.511Mev pulses. The gate generator receives the logic pulse and adjusts the width to gate the analog 511 keV pulses from detector number 2 through the multi channel analyzer. As the logic pulse generated by the gate generator reaches the multi channel analyzer it triggers the multi channel analyzer gate which when receiving a positive signal in data port number 2 allows the signal in data port number one to pass through. However, when the data port number 2 is receiving no positive square wave signal the multi channel analyzer will not collect the signal that is being sent to data port number one.

Chapter 3

Preliminary Measurements

3.1 Detector Energy Resolution

The energy resolution of the NaI detectors were measured and calculated. The energy resolution was found by first measuring an energy spectrum of a source emitting gamma rays of a known energy. By dividing the width of the energy peak (the number of channels wide) at half its height by the channel number that corresponds to the energy of the radiation being collected the energy resolution of the detector is approximately obtained. Both detectors collected the energy spectrum of Na-22 and using this spectrum the energy resolution of the detectors was found. Detector number one had a peak full width at half the peak max height of 33 channels. The 511 keV energy radiation being collected corresponded to channel number 389. So, the energy resolution of the detector is 33/389 = 8.4%. Detector number two had a peak width of 40 channels where the 511 keV radiation being collected corresponded to channel 420. So, the energy resolution of this detector is 40/420 = 9.5%.

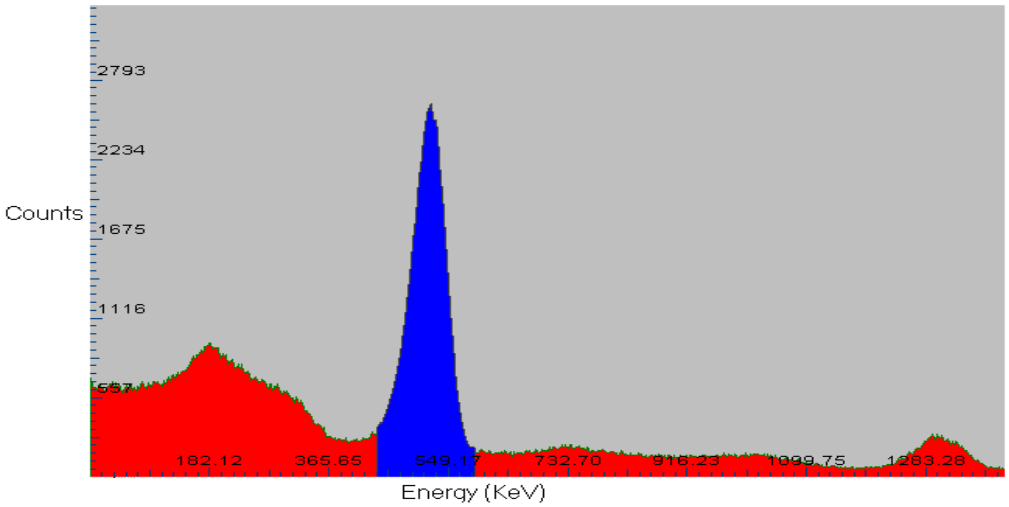

Fig. 3.1.1 Energy spectrum collected to find the energy resolution of detector #1. The peak in blue is the 511 keV data

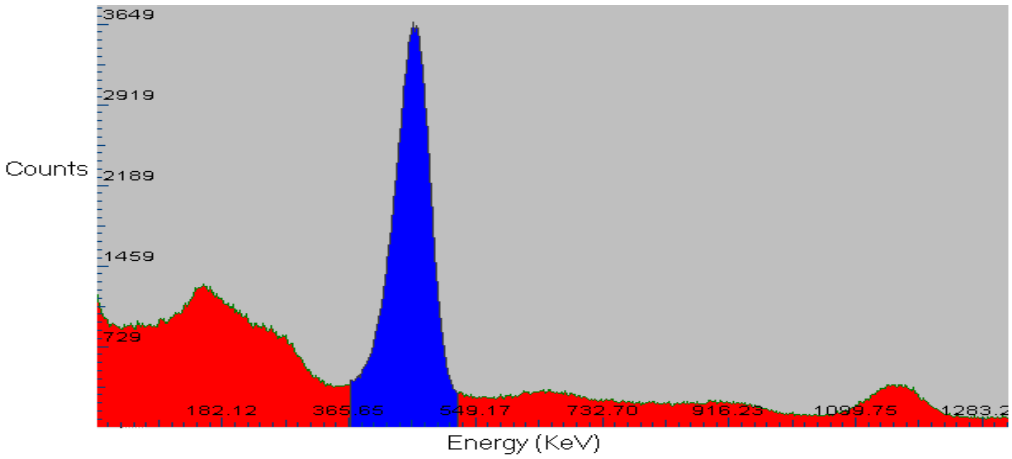

Fig 3.1.2 Energy spectrum collected to find the energy resolution of detector #2

3.2 Background Reduction

By collecting a Na-22 spectrum both with and without the coincidence electronics a comparison can be made that will help evaluate the efficiency of the background reduction technique that has been implemented. The background radiation can be observed to be reduced by at least ½. With the presence of the Na-22, 511 keV annihilation photons are constantly triggering the gate and allowing not only the transmitted annihilation photon to enter the data spectrum but also other radiation that may happen to enter the detector in coincidence with the triggering 511 keV annihilation photon. By collecting an energy spectrum without using the NIM electronics to reduce background events the average number of background events per channel was found. Then the same spectrum was collected with NIM electronics and the average background events per channel compared. However, when the Na-22 is replaced with another radiation source that does not emit 511 keV annihilation photons there is an evident reduction in collected data.

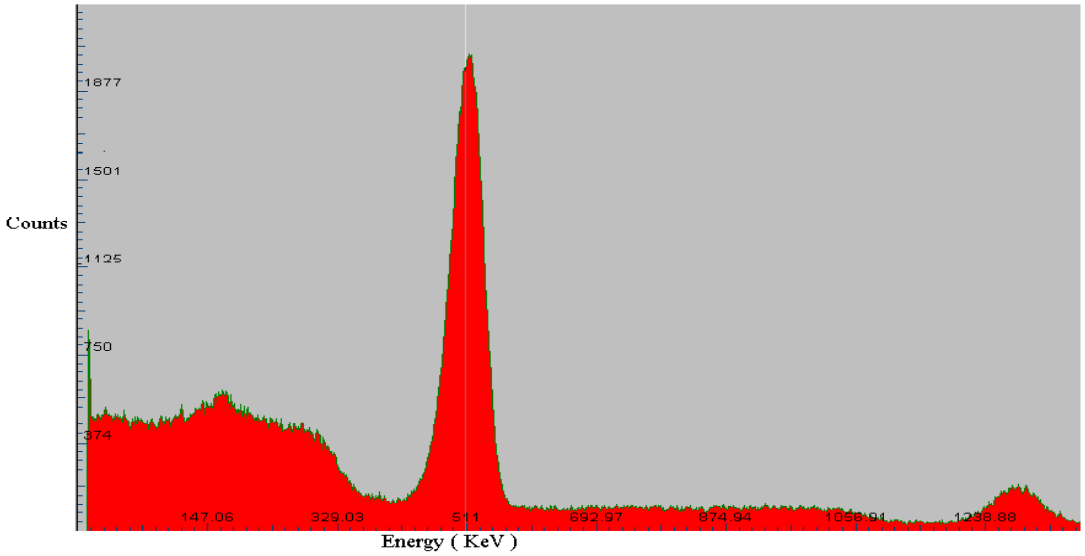

Fig 3.2.1 Na-22 spectrum taken requiring coincidence between detectors. The number of background events is reduced while the desirable data remains with little reduction.

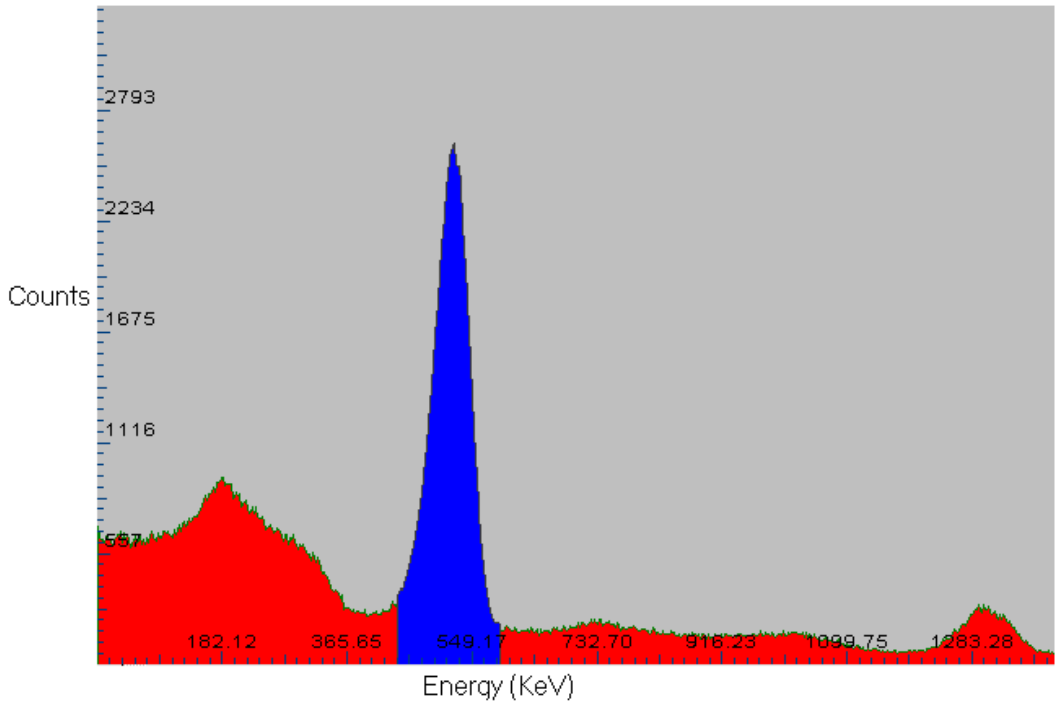

Fig 3.2.2 Na-22 spectrum taken not requiring coincidence between detectors

When a Co-60 spectrum is taken without the use of the coincidence electronics there are two very evident peaks at 1.17 MeV and 1.33 MeV, the energies of the two Co-60 gamma rays. However, when the electronics require coincidence with a 511 keV annihilation photon the spectrum of Co-60 is nearly eliminated.

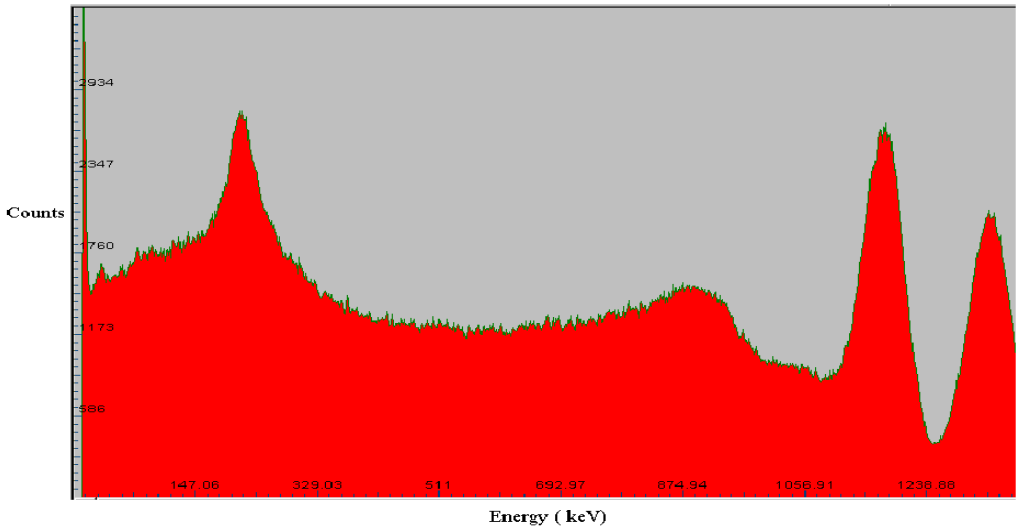

Fig 3.2.3 Co-60 spectrum taken not requiring coincidence between two detectors

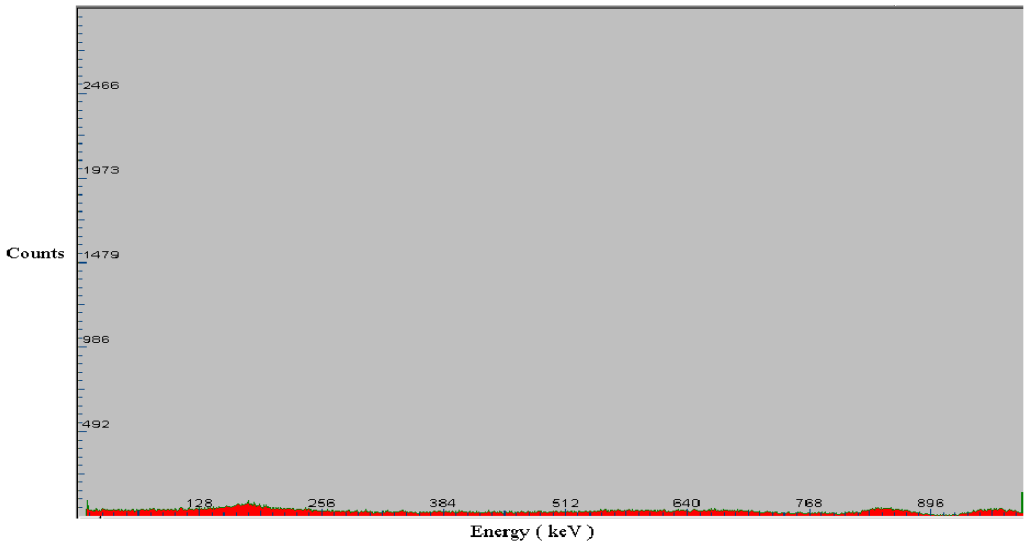

Fig 3.2.4 Co-60 spectrum taken requiring coincidence between two detectors

The coincidence electronics have also been tested for the case where an attenuating object is being transmitted. The objects being transmitted through are 0cm, 5cm, 10cm and 13cm of water at a source distance from the data detector of 20cm. Each has been tested for the case using the coincidence and not using the coincidence in order to compare the efficiency of the background reduction. The following spectra represent the data taken. Each data set was taken with the source at 20 cm from the data detector and 1 cm from the coincidence detector. There was a 1 cm collimator directly between the source and the coincidence detector. This was done to help restrict the coincidence detector to cause a trigger only for the annihilation photons in the beam line.

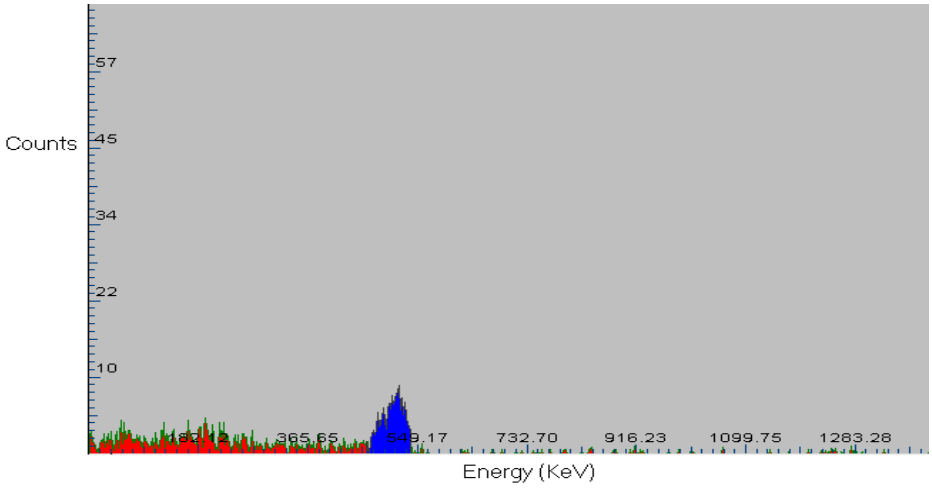

Fig 3.2.5 Na-22 spectrum taken requiring coincidence between two detectors data was collected for 500 seconds through 0cm of water.

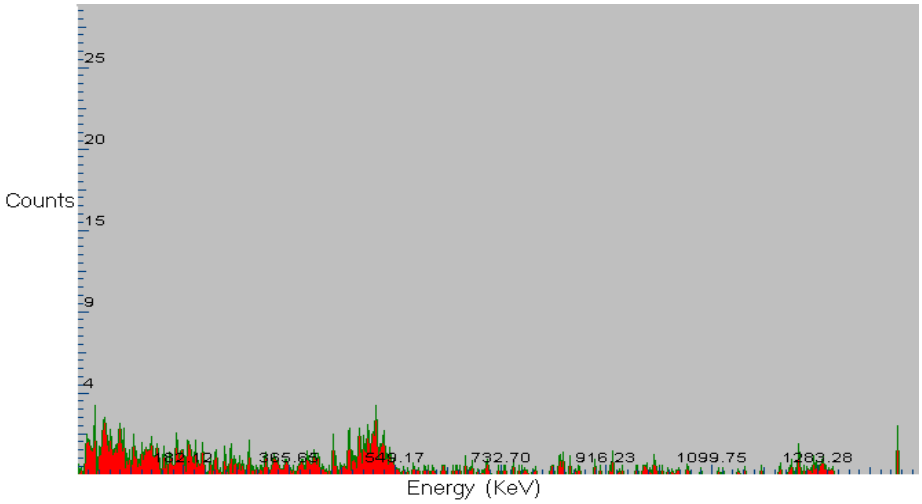

Fig 3.2.6 Na-22 Spectrum taken requiring no coincidence with data being collected for 500 seconds through 0cm of water.

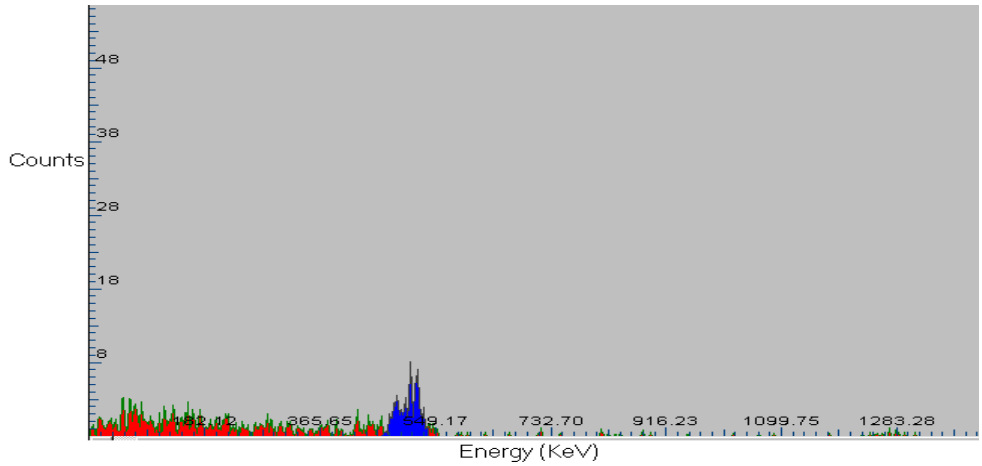

Fig 3.2.7 Na-22 spectrum taken requiring coincidence between two detectors and being attenuated through 5cm of water

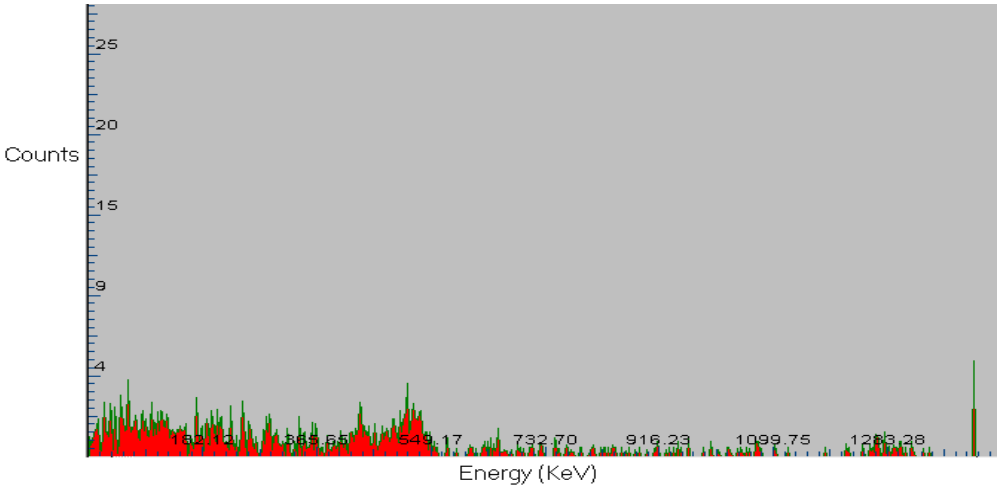

Fig 3.2.8 Na-22 spectrum taken requiring no coincidence between detectors and being attenuated through 5 cm of water.

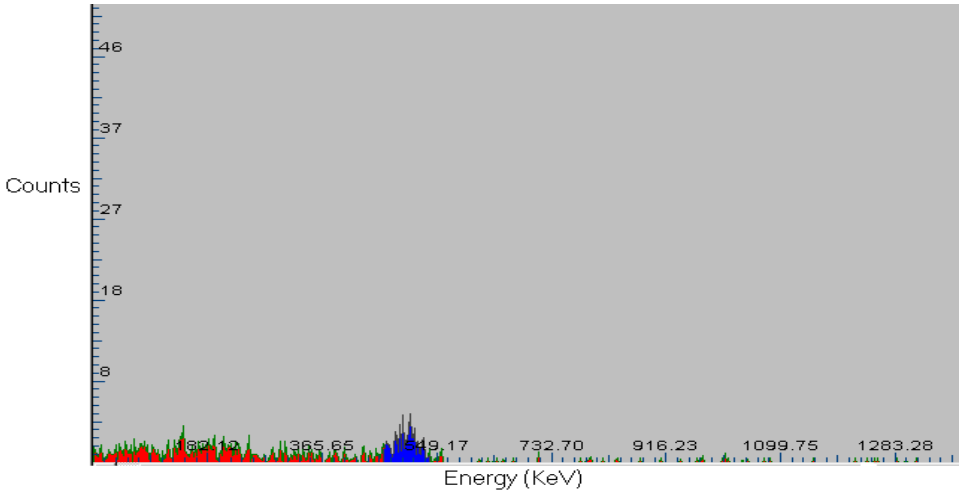

Fig 3.2.9 Na-22 spectrum taken requiring coincidence between two detectors and being attenuated through 10cm of water.

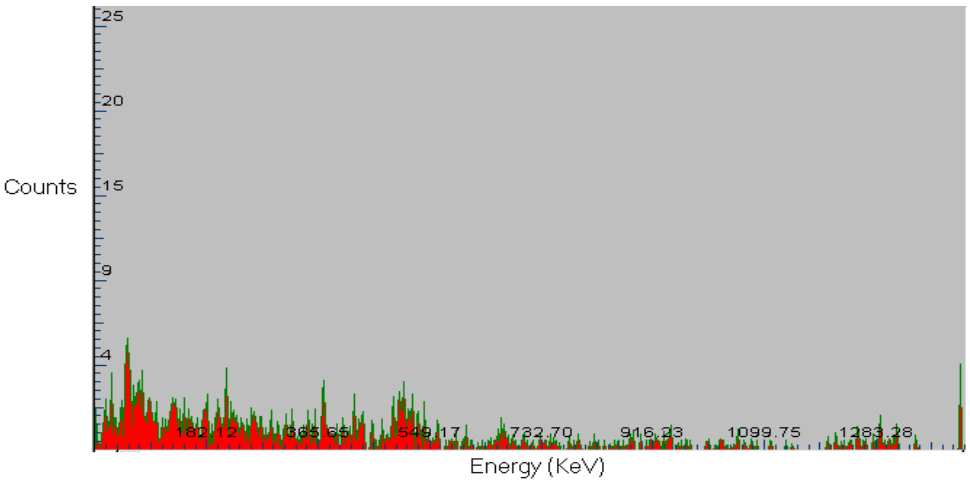

Fig. 3.2.10 Na-22 data taken not requiring coincidence between two detectors and being attenuated by 10cm of water.

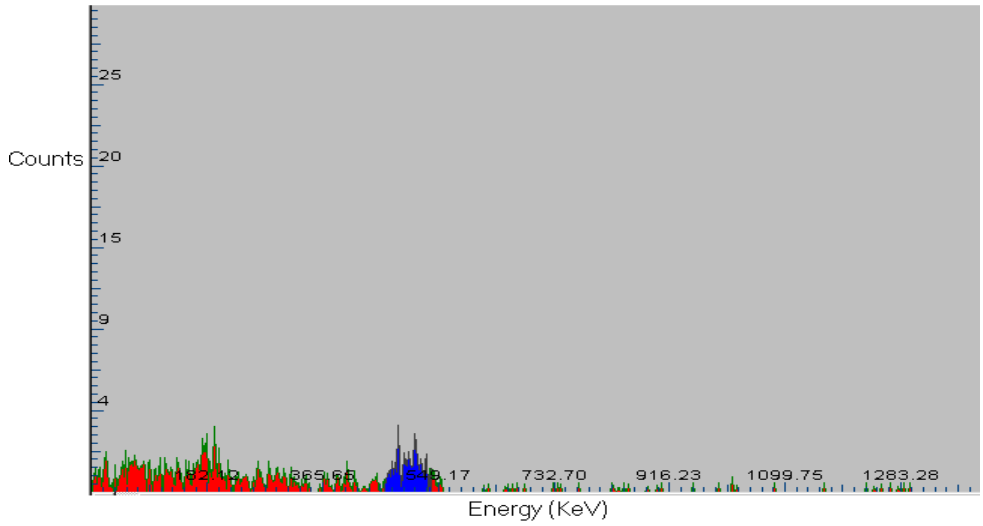

Fig 3.2.11 Na-22 spectrum taken requiring coincidence between two detectors and being attenuated through 13cm of water.

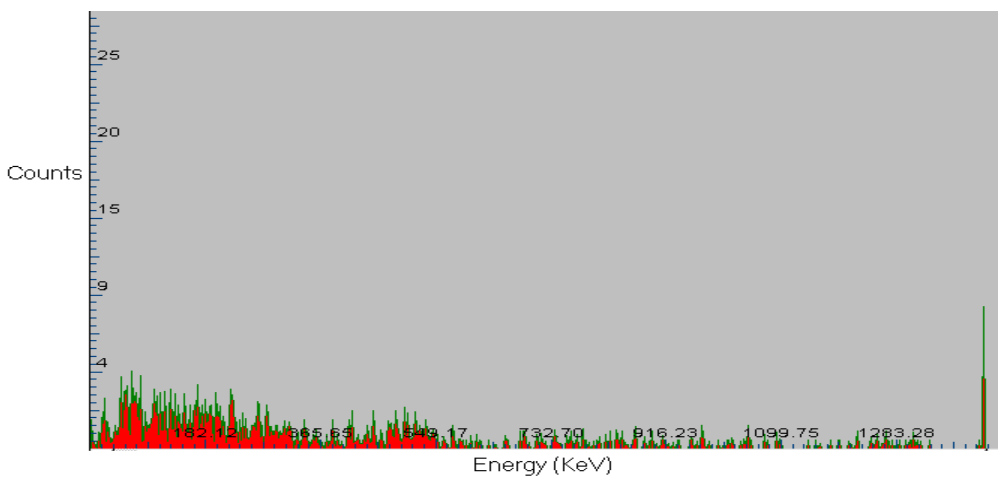

Fig. 3.2.12 Na-22 spectrum taken not requiring coincidence between two detectors and being attenuated through 13cm of water.

Knowing that the attenuation due to distance through the material is exp[- μ x] where x is the distance, we can use some of the preceding data to find the measured

attenuation coefficient for water. The slope of the graph Ln[count rate] Vs distance will be the our measured attenuation coefficient of water.

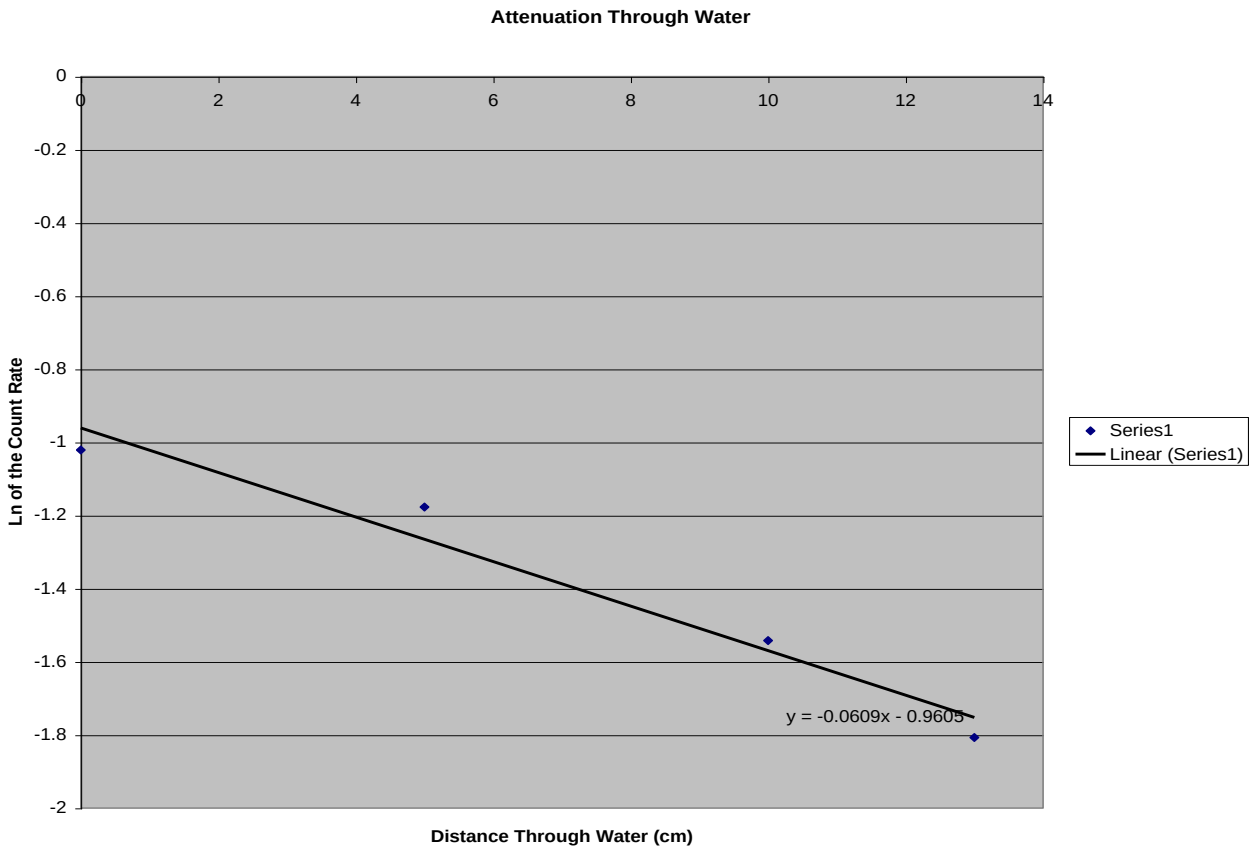

Fig 3.2.13 A graph of Ln(count rate) Vs distance through water. The slope of this graph is the measured attenuation coefficient for water using the data from preceding coincidence measurements.

The slope of this graph is approximately .06 therefore the measured attenuation coefficient of water is $.06cm^{-1}$.

3.3 Collimator Efficiency

Data was taken in order to measure how effective the collimator was at narrowing the incident annihilation photons to a narrow beam. This measurement was done by scanning the radiation source across the intended beam line and collecting radiation spectrums at particular points along the scan. The Na-22 radiation source was placed 20 cm away from the transmitted beam detector and was then placed 10 cm out of alignment with the collimator. Data was collected on 1 cm increments from 10 cm out of alignment, to alignment and then out to –10 cm out of alignment. By measuring the beam intensity at each point the effectiveness of the collimator can be found. We would expect that in a good collimator the beam intensity will be very low at 10 cm out of alignment and will slowly grow more intense the closer to alignment that the radiation source becomes. At the point of alignment a good collimator would show a spike in beam intensity. The data collected did show that this was true of this collimator.

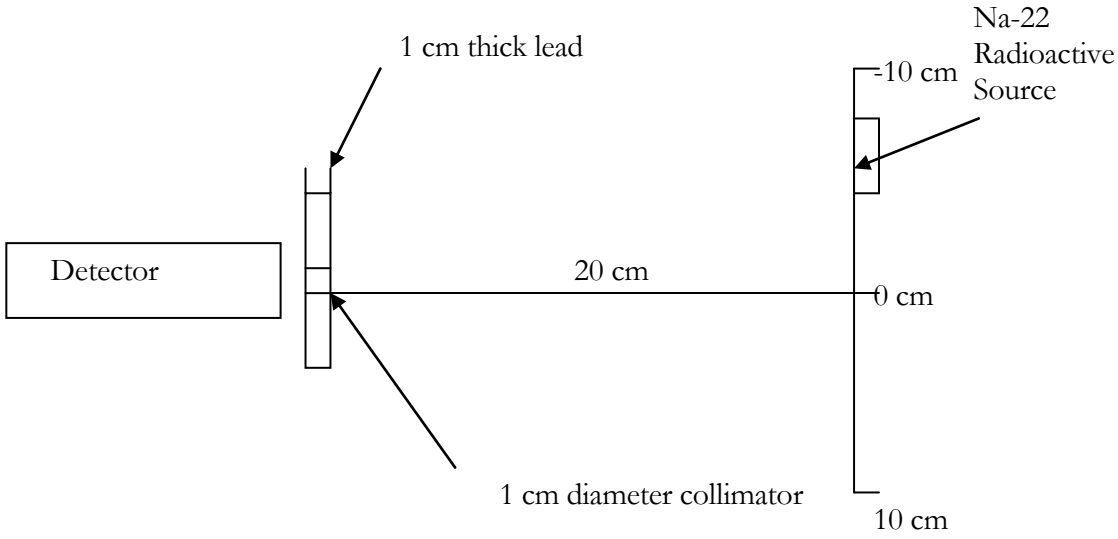

Fig 3.3.1 Figure demonstrating alignment data collection procedure for sensitivity to source, collimator, detector alignment.

The collimation could also be achieved by using the combination of the coincidence detector and data detector. Geometrically the radiation source emits the annihilation photons out radially. Using this fact we can collimate the beam without having to use a lead collimator. Since the data will not be collected without coincidence between the data detector and the coincidence detector we could place the coincidence detector a certain distance behind the source so that geometrically the only annihilation photons that are collected by the data detector are those that fall on a 1cm circle. Here a picture will be very helpful for explanation.

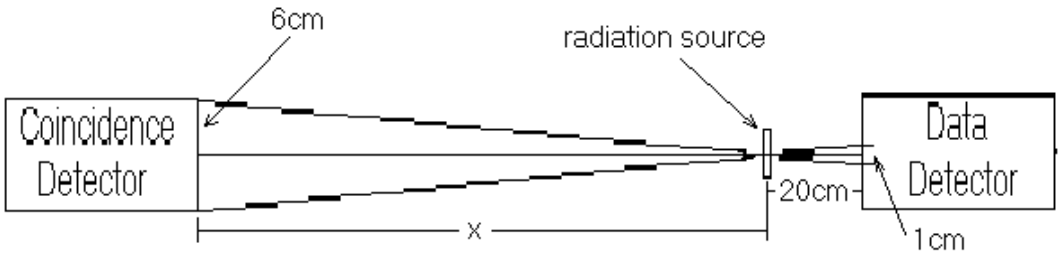

Fig 3.3.2 Figure demonstrating the use of geometric collimation.

Since the collimator diameter is 1cm and the distance from the source to the data detector is 20 cm the distance from the source to the coincidence detector can be found using a proportion. $\frac{1}{20} = \frac{6}{x}$ Solving for x, x = 120cm. So by placing the coincidence detector 120cm behind the radiation source the annihilation photon beam can be effectively collimated electronically. Geometric collimation would also reduce the number of data collections out of beam line since the coincidence detector would only be able to receive data photons. This method can be compared to the lead collimation method by collecting a set of spectrums using both methods and comparing the count rates.

3.4 Data Collection Time

Data collection time in this case, is mostly dependent on the amount of time it will take to collect enough data for each measurement in order to acquire a particular amount of error for that data. While measuring the number annihilation photons there

is a statistical error that is equal to the square root of the number of counts you have collected. This project requires ten percent statistics, therefore each measurement will require one hundred counts in order to achieve this. The number of gamma detections can be calculated using a formula given particular experiment conditions. Calculations will be made using conditions of a one micro-Curie Na-22 source, the object being scanned will be a cylindrical bottle of water with a diameter of 10cm, and the desired resolution will be .5 cm. The number of gamma detections cam be calculated using the formula.

$$\text{Number Detected} = Ndis \bullet \left[\left(\frac{\Delta\Omega}{4\Pi} \right) (\varepsilon_1)(\varepsilon_2)(C_1)(C_2) e \exp[-\mu x] \right] \quad (3.1)$$

Where Ndis is the number of disintegrations in the nucleus resulting in at least one gamma emission, $\frac{\Delta\Omega}{4\Pi}$ is the geometric solid angle of the detections, ε_1 and ε_2 are the detector efficiencies of detector number 1 and detector number 2, C_1 and C_2 are the photopeak fractions of both detectors where the photopeak fraction is the fraction of all interacting events that produce a full photopeak with energy o 511 keV, μ is the coefficient of attenuation for the material being scanned and x is the distance through which the annihilation photons have to travel. The detector efficiency for both detectors was calculated where μ is the attenuation of the NaI detector crystal and L is the length of the detector crystal. The attenuation coefficient μ for NaI is .41 $\frac{1}{cm}$ and the length L of the crystal is 2.54 cm.

$$\varepsilon_1 = \varepsilon_2 = 1 - \exp\left[-(\mu)(L) \right] \quad (3.2)$$

$$\varepsilon_1 = \varepsilon_2 = 1 - \exp\left[-\left(.41\frac{1}{\text{cm}} \right)\left(2.54 \text{ cm} \right) \right] \quad (3.3)$$

$$\varepsilon_1 = \varepsilon_2 = .64 \quad (3.4)$$

Data was collected to find the number of counts lost to the escaping Compton interaction, this was found to be 61% therefore 39% of the annihilation photons that interact in the detector will be collected as having 511 keV energies. The Ndis or number of disintegrations per second for a 1 microcurie Na-22 source will be $3.7 \bullet 10^4$ disintegrations/sec. $\Delta\Omega$ must be calculated.

$$\Delta\Omega = \frac{\text{Area}}{\text{distance}^2} \quad (3.5)$$

$$Area = \Pi r^2 \quad (3.6)$$

$$\text{distance} = 11\text{cm} \quad (3.7)$$

Since the resolution is .5 cm the radius of the area will be .25cm.

$$\Delta\Omega = \frac{\Pi .25^2}{11^2} \quad (3.8)$$

$$\frac{\Delta\Omega}{4\Pi} = \frac{1}{7744} \quad (3.9)$$

The attenuation coefficients of the materials that the beam will be traveling through will add to give the attenuation coefficient μ that is used in the equation. μ can be found by adding the coefficient of attenuation for each material multiplied by the distance through which the beam travels through the material. The beam will be traveling through both air and water. The attenuation coefficient for water is

$9.687\times10^{-2}\frac{1}{cm}$ and the attenuation coefficient for air is $.00011\frac{1}{cm}$. The beam will be traveling through 8.167cm of water on average and 1 cm of air.

$$\mu x = 9.687\times10^{-2}\frac{1}{cm}\bullet(8.167cm)+.00011\frac{1}{cm}\bullet 1cm \quad (3.10)$$

This will give a number detected to be.

$$\text{Number Detected} = Ndis\bullet\left[\left(\frac{1}{7744}\right)(.64)(.64)(.39)(.39)e\exp[-\mu x]\right] \quad (3.11)$$

$$\text{Number Detected} = \left(3.7\times10^{4}\frac{\text{Disintigrations}}{\text{Second}}\right)\bullet\left(\frac{1}{7744}\right)(.64)(.64)(.39)(.39)e\exp\left[-(.7912\frac{1}{cm})\right]$$

(3.12)

$$\text{Number Detected} = .1349\ \frac{\text{Detections}}{\text{Second}} \quad (3.13)$$

Each measurement will require 100 detections, so the average time that will be required for each measurement can be found using a proportion.

$$\frac{.1349\text{ Detections}}{1\text{ Second}} = \frac{100\text{ Detection}}{x\text{ Seconds}} \quad (3.14)$$

$$x = 741.152\text{ Seconds} \quad (1.15)$$

Each measurement will require 741.152 seconds. Next the number of required measurements must be found. Since the collimator in this case has a one half

centimeter diameter, the transmitting beam will be one half centimeter across. Therefore, 20 translations will be required to completely cover the 10 cm diameter body of water.

Next the number of rotations required for this particular setup will be determined. In a higher resolution scanner there would be one rotation for every degree in a half circle, in other words there would be 180 rotations. However since the width of the beam in this case is larger it will require more rotation per angle in order to avoid overlap, therefore there will be required fewer rotations to cover the 180 degrees around the object. At this point an illustration will be helpful.

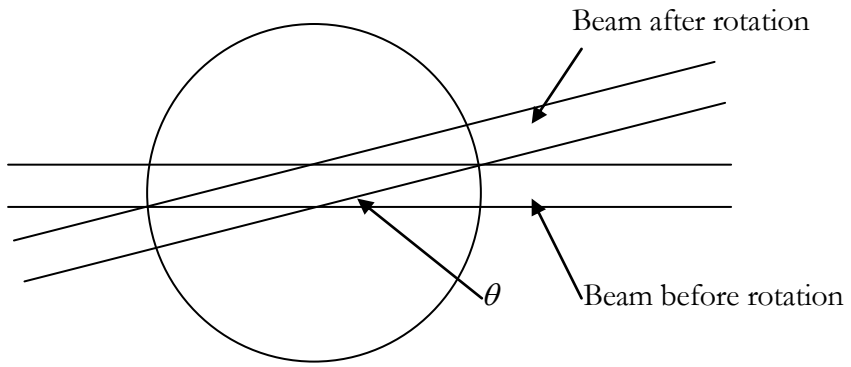

Fig 3.4.1 Picture describing the rotation required to avoid overlapping beam paths.

.

This picture shows that a beam rotated by the angle theta will allow data to be collected without unnecessary overlap. Knowing that the radius of the object is 5 cm and the beam width is $\frac{1}{2}$ cm the angle theta can be calculated.

$$\sin(\theta) = \frac{\frac{1}{2}}{5} = \frac{1}{10} \quad (3.16)$$

$$\sin^{-1}\left(\frac{1}{10}\right) = 5.74^{o} \quad (3.17)$$

Since the beam angle will be rotated 5.74 degrees it will require $\left\lceil \frac{180}{5.74} \right\rceil$ = 32 rotations. Since every rotation will be accompanied by 20 translations and therefore 20 measurements there will be $32 \times 20 = 640$ measurements made in the scan. The approximate time for each measurement has already been calculated to be 741.152 seconds the scan will require $741.152 \times 640 = 474337 \text{ Seconds}$. This is equal to 131.76 hours or five and one half days of continuous scanning.

Chapter 4

Conclusion

4.1 Summary and Observations

The plausibility of constructing this novel design Computed Tomography Scanner has been investigated first by exploring the history of scientific discoveries pertaining to Computed Tomography and CT design.

With the discovery of x-rays and their properties the concept of internal imaging suddenly became a reality and with the publication and widespread popularity of the discovery advances in image construction using radiology quickly developed. The common use of radiology in internal imaging revealed certain drawbacks in diagnostics using the method so the search for a new method began. Through the work of multiple scientists and mathematicians of different fields, the foundations for projection set 3-D image reconstruction were formed and the base upon which theoretical Computed Tomography would stand was constructed.

The theory of Computed Tomography deals with the way in which a material will attenuate a beam of photons that is passing through it. The three interaction mechanisms by which a material will remove photons from a beam are the Compton effect, the photo-electric effect and pair production. The frequency at which these interaction mechanisms occur in a material to remove photons from a beam of a particular energy is called the attenuation coefficient. The different materials in a body being observed using x-rays for example will attenuate the beam more or less

depending upon the type of material. This characteristic allows an image to be produced of the different materials spread throughout the body due to their identification using the beam attenuation. A Computed Tomography Scanner uses this information and projections sets to calculate the attenuation coefficient at many points in a body and therefore produce an image on a computer screen using the spread of attenuation coefficient points.

The mechanical setup of the novel design scanner has two inline detectors with an annihilation photon radiation source used as the photon emitter for projection sets. The object being imaged is rotated and translated between the detectors and radiation source in order to obtain the data required to calculate the attenuation at any point in the object and therefore construct an image. The electronics setup uses a coincidence of data from the radiation source between the two detectors to reduce the collected background radiation and allow more significant data to be collected.

Preliminary measurements were taken to begin construction of the novel design. First the energy resolution of both detectors was found to be 8.4% for detector number one and 9.5% for detector number two. Data was also taken to demonstrate the success of coincidence electronics in filtering out background noise from the data collection. Data was then collected to show the attenuation of annihilation through different measures of water.

The collimation methods were tested and calculated for both geometric and lead collimation.

It is also important to find the time it will take to complete a scan using the novel design. Through a series of calculations it was found that a complete scan using the condition described would theoretically take 131.76 hours.

1 T.S Curry, J.E. Dowdy, R.C. Murry, Christensen's Physics of diagnostic radiology (1990).

2 T.S Curry, J.E. Dowdy, R.C. Murry, Christensen's Physics of diagnostic radiology, 289 (1990).

3 S. Webb, The Physics of Medical Imaging (1988).

4 S. Webb, The Physics of Medical Imaging, 10 (1988).

5 M.R. Wehr, J.A. Richards Jr., T.W. Adair III, Physics of the Atom (1978).

6 P.A.Tipler,R.A.Llewellyn Modern Physics (1999).

7 M.R. Wehr, J.A. Richards Jr., T.W. Adair III, Physics of the Atom (1978).

8 W.E. Burcham, Elements of Nuclear Physics, (1979)

9 M.R. Wehr, J.A. Richards Jr., T.W. Adair III, Physics of the Atom (1978).211-215

10 M.R. Wehr, J.A. Richards Jr., T.W. Adair III, Physics of the Atom (1978).211-215

11 M.R. Wehr, J.A. Richards Jr., T.W. Adair III, Physics of the Atom (1978).211-215

12 W.R.Hendee,E.R.Ritenour, Medical Imaging Physics, 253 (2002).

13 S. Webb, The Physics of Medical Imaging, 106-115 (1988).

14 S. Webb, The Physics of Medical Imaging, 106-115 (1988).

15 M.R. Wehr, J.A. Richards Jr., T.W. Adair III, Physics of the Atom (1978).

16 W.E. Burcham, Elements of Nuclear Physics, 128 (1979).

17 A.R.Foster, R.L.Wright Jr., Basic Nuclear Engineering, 127 (1977).